The variations of VOCs based on the policy change of Omicron in traffic-hub city Zhengzhou

Bowen Zhang[1, 3], Dong Zhang[2, 3], Zhe Dong[2, 3], Xinshuai Song[1, 3], Ruiqin Zhang[1, 3], Xiao Li[1, 3,*]

[1]School of Ecology and Environment, Zhengzhou University, Zhengzhou 450001, China

[2]College of Chemistry, Zhengzhou University, Zhengzhou 450001, China

[3]Institute of Environmental Sciences, Zhengzhou University, Zhengzhou 450001, China

Correspondence to: Xiao Li, E-mail address: lixiao9060@zzu.edu.cn

Abstract: Online volatile organic compounds (VOCs) were monitored before and after the Omicron policy change at an urban site in polluted Zhengzhou from December 1, 2022, to January 31, 2023. The characteristics and sources of VOCs were investigated. The daily mean concentrations of $PM_{2.5}$ and total VOCs (TVOCs) ranged from 53.5 to 239.4 µg/m³ and 15.6 to 57.1 ppbv, respectively, with mean values of 111.5 ± 45.1 µg/m³ and 36.1 ± 21.0 ppbv, respectively, throughout the period. Two severe pollution events (designated as Case 1 and Case 2) were identified in accordance with the National Ambient Air Quality Standards (NAAQS) (China's National Ambient Air Quality Standards (NAAQS) from 2012). Case 1 (December 5 to December 10, $PM_{2.5}$ daily mean = 142.5 µg/m³) and Case 2 (January 1 to January 8, $PM_{2.5}$ daily mean = 181.5 µg/m³) occurred during the infection period (when the policy of "full nucleic acid screening measures" was in effect) and the recovery period (after the policy was cancelled), respectively. The $PM_{2.5}$ and TVOCs values for Case 2 are, respectively, 1.3 and 1.8 times higher than those for Case 1. The results of the positive matrix factor modeling demonstrated that the primary source of volatile organic compounds (VOCs) during the observation period was industrial emissions, which constituted 32% of the total VOCs, followed by vehicle emissions (27%) and combustion (21%). In Case 1, industrial emissions constituted the primary source of VOCs, accounting for 32% of the total VOCs. In contrast, in Case 2, the contribution of vehicular emission sources increased to 33% and became the primary source of VOCs. The secondary organic aerosol formation potential for Case 1 and Case 2 were found to be 37.6 µg/m³ and 65.6 µg/m³, respectively. In Case 1, the largest contribution of SOAP from industrial sources accounted for the majority (63%, 23.8 µg/m³), followed by vehicular sources (18%).

34 After the end of the epidemic and the resumption of productive activities in the society,

35 the difference in the proportion of SOA generated from various sources decreased. Most

36 of the SOAP came from solvent use and fuel evaporation sources, accounting for 32%

37 (20.9 μg/m³) and 26% (16.8 go/m³), respectively. On days with minimal pollution,

38 industrial sources and solvent use remain the main contributors to SOA formation.

39 Therefore, regulation of emissions from industry, solvent-using industries and motor

40 vehicles need to be prioritized to control the $PM_{2.5}$ pollution problem.

41

42 **Keywords: Volatile organic compounds; Pollution episode; Source apportionment; Positive**

43 **Matrix Factorization model; Secondary organic aerosol formation potential;**

1. Introduction

Volatile organic compounds (VOCs) in the atmosphere have high reactivity and can react with nitrogen oxides (NO_x) to form a series of secondary pollutants such as ozone (O_3) and secondary organic aerosol (SOA), resulting in regional air pollution (Li et al., 2019; Hui et al., 2020). The problem of O_3 pollution has been plaguing major urban agglomerations in China (Zheng et al., 2010; Li et al., 2014; Wang et al., 2017). SOA is an important component of fine particulate matter ($PM_{2.5}$) and contributes significantly to haze pollution (Liu et al., 2019). $PM_{2.5}$ remains the most significant air pollutant in many Chinese cities for years (Shao et al., 2016; Wu et al., 2016). In addition, VOCs, represented by the benzene homologues, can cause damage to kidneys, liver, and nervous system of humans when they enter the body (Zhang et al., 2018).

Studies have shown that the most common VOC components in China are alkanes, olefins, aromatic hydrocarbons, oxygenated VOCs (OVOCs), and halogenated hydrocarbons, among which alkanes are the most abundant species (Liu et al., 2020; Zhang et al., 2021a). VOCs in the atmosphere have a wide range of sources, and VOCs in different regions are affected by multiple factors such as local geography, climate, and human activities (Mu et al., 2023; Zou et al., 2023). The above reasons lead to significant regional and seasonal differences in the characteristics of VOCs (Song et al., 2021). For example, the annual average concentration of VOCs in the coastal background area of the Pearl River Delta is 9.3 ppbv. The seasonal variation trend of VOCs is high in autumn and winter and low in summer (Yun et al., 2021). In contrast, the average VOC concentration in autumn and winter in Beijing was 22.6 ± 12.6 ppbv, and the VOC concentration in the winter heating period was twice that in the autumn non-heating period (Niu et al., 2022).

Moreover, the sources of VOC components in different regions are also related to the local industrial structure and living habits. In rural areas of North China Plain in winter, it is found that the SOA formation potential (SOAP) of VOCs under low NO_x conditions is significantly higher than that under high NO_x conditions, and the increase of aromatic hydrocarbon emissions caused by coal combustion is the main reason for the higher SOAP in winter (Zhang et al., 2020). Li et al. (2022) found that the average increased concentration of acetylene was 4.8 times from autumn to winter in the Guanzhong Plain, indicating that fuel combustion during the heating period in winter has a significant impact on the composition of VOCs. In contrast, continuous

observations conducted by Zhou et al. (2022) in the suburbs of Dongguan in summer found that industrial solvent usage, liquefied petroleum gas (LPG) and oil and gas volatilization were the main sources of VOCs. The results highlighted a wide variation of characteristics, sources and chemical reactions of VOCs in the atmosphere thus it is necessary to investigate VOCs in different cities when formulating control measures.

Zhengzhou, as the capital of Henan Province, is an important transportation hub and economic center in the Central Plains region. Zhengzhou is currently facing significant air pollution problems, with the Air Quality Index at the bottom of the national ranking of 168 cities for many years. In January 2023, for example, the number of polluted days with $PM_{2.5}$ as the primary pollutant was 17, and the daily average value of $PM_{2.5}$ reached a maximum of 298 $\mu g/m^3$ (https://www.aqistudy.cn/historydata/daydata.php?city=%E9%83%91%E5%B7%9E &month=202301, Accessed Jan 2024), which is almost 300% higher than the Chinese daily average standard (grade II, 75 $\mu g/m^3$). The studies of VOCs were carried out in Zhengzhou in recent years, which focused on the characteristics and sources of VOCs during pollution episodes (Lai et al., 2024) or before the coronavirus epidemic outbreak (Li et al., 2020; Zhang et al., 2021b). While some atmospheric VOCs studies involving the impact of Covid-19 lockdown have been performed in India (Singh et al., 2023a), in China (e.g., Pei et al., 2022; Jensen et al., 2023; Zuo et al., 2024), or with respect to toluene, benzene, m/p-xylene and ethylbenzene only (e.g., Sahu et al., 2022; Singh et al., 2023b), a gap persisted in the investigation of VOCs due to the impact of abolishment of China's zero-policy. Furthermore, some studies have discussed the impact of changes in human production activities on air pollution during and after the outbreak of the coronavirus disease (e.g., Ma et al., 2022; Jiang et al., 2023; Song et al., 2023), but as mentioned earlier, only a few studies with in-depth exploration of the changes in VOCs and none dealing with ending the zero-Covid policy during Omicron variant infection period.

In this study, we conducted continuous online observations of VOCs during the polluted winter season at an urban site in Zhengzhou. The study covered the period following the removal of lockdown measures. We focused on pollution events when the daily average $PM_{2.5}$ concentration exceeded 75 $\mu g/m^3$ (China's Class II standard) for more than three consecutive days. Days with $PM_{2.5}$ concentrations below 35 $\mu g/m^3$ (China's Class I standard) were classified as clean days. During this period, China lifted zero-COVID strategies, announcing the '10 measures' for optimizing COVID-19 rules

on December 7, 2022 (http://www.news.cn/politics/2022-12/07/c_1129189285.htm, Accessed Jan 2024). Zhengzhou's epidemic prevention and control measures changed with the issuance of Circular No. 163 on December 4, 2022, which allowed the reopening of closed public places. As a result, movement within Zhengzhou increased and social production resumed. Our research specifically examines the period dominated by the COVID-19 Omicron variant. where they demonstrate notable differences from the early virus strains (i.e., original SARS-CoV-2 virus and Delta) in terms of geographical transmission, the scale of the infected population, and symptom manifestation (Petersen et al., 2022; Merino et al., 2023).

After the quarantine policy was lifted, people basically rested at home due to infection or fear of infection with Omicron. The resumption of normal production and life depends on herd immunization. This outbreak event is the longest in duration and the largest in number of infections since the 2020 outbreak of the novel coronavirus in Zhengzhou. It would be beneficial to investigate the impact of this event on emissions related to transportation and industrial production. This change is worth exploring in terms of its impact on transportation and industrial production emissions. Therefore, the characteristics and variations of VOCs during different periods were investigated to assess their impact on the formation of SOA and to provide data support for future pollution control policies in Zhengzhou.

2. Materials and methods

2.1 Sample collection and Chemical analysis

The online VOCs observation station is located on the roof of the Zhengzhou Environmental Protection Monitoring Center, which is in the urban area. The sampling site is close to main roads on three sides (150 m away from Funiu Road on the east side, 200 m away from Qinling Road on the west side, and connected to Zhongyuan Road on the south side), and surrounded by residential areas and commercial areas without other large nearby stationary sources. The sampling period for this study was from December 1, 2022, to January 31, 2023, and serious $PM_{2.5}$ pollution in Zhengzhou was of frequent occurrence during December and January. (https://www.aqistudy.cn/historydata/monthdata.php?city=%e9%83%91%e5%b7%9e #:~:text=%E7%94%9F%E5%91%BD%E6%9D%A5%E6%BA%90%E8%87%AA% E7%84%B6%EF%BC%8C%E5%81%A5). Apart from a brief occurrence of rain and snow on December 25, the sampling days were either sunny or cloudy. The wind speed (WS), temperature (Temp) and relative humidity (RH) during this period were 1.3 ± 0.9 m/s, 5.3 ± 3.2 ℃ and $38.9 \pm 19.0\%$), respectively, similar to the values observed in previous years in Zhengzhou. It is interesting to point out that the sampling period in the present study covered the entire infection period of Omicron in Zhengzhou, including the phase of surge in infected population (Infection period, from 2022.12.01 to 2022.12.31) and restoration of production and livelihood phase (Recovery period, from 2023.1.1 to 2023.1.31 in 2023) (Fig. S1, Chinese Center for Disease Control and Prevention, 2023).

The VOCs were measured hourly using a GC-FID/MS (TH-PKU 300 b, Wuhan Tianhong Instruments Co., China). The instrument TH-PKU300b includes electronic refrigeration ultra-low temperature pre-concentration sampling system, analysis system and system control software. The ambient VOCs in the first 5 minutes of each hour were collected by the sampling system and then entered the concentration system. Under low temperature conditions, the VOCs samples collected were frozen in the capillary capture column, and then quickly heated and resolved, so that the compounds entered the analysis system. After separation by chromatographic column, the compounds were monitored by FID and MS detectors. During the detection process, the atmospheric samples collected undergo analysis through two distinct pathways. C2-C5 hydrocarbons are analyzed using FID, while C5-C12 hydrocarbons, halocarbons,

164 and OVOCs are analyzed with a MS detector. After excluding species with missing data
165 exceeding 10%, the detected volatile organic compounds include 29 alkanes, 11 alkenes,
166 17 aromatics, 35 halocarbons, 12 OVOCs, 1 alkyne (acetylene), and 1 sulfide (CS_2)
167 with a total of 106 compounds. A detailed description of the instrumentation can be
168 found in our previous study (Zhang et al., 2021b; Shi et al., 2022; Zhang et al., 2024).

169   The instrument was calibrated per week to ensure the accuracy of VOCs by
170 injecting standard gases with a five-point calibration curve. The detection limit of C2-
171 C5 hydrocarbons ranges from 0.007 to 0.099 ppbv, other hydrocarbons are 0.004–0.045
172 ppbv, halogenated hydrocarbons 0.009-0.099 ppbv, OVOCs and other compounds of
173 0.006–0.095 ppbv. Thirty-two of the monitored VOCs had over 90% observed data
174 greater than the detection limit, and 34 had more than 50% observed data greater than
175 the detection limit.

176   Simultaneous observations at the same site were also carried out for particulate
177 matter ($PM_{2.5}$, PM_{10}), other trace gases (carbon monoxide (CO), O_3, nitric oxide (NO),
178 nitrogen dioxide (NO_2)), and meteorological data (Temperature, RH, WS, and wind
179 direction (WD)) based on 1 h resolution.

2.2 Positive Matrix Factorization (PMF) model

181   EPA PMF5.0 model was used for the quantitative source analysis of VOCs (Norris
182 et al., 2014). The principles and methods have been described in detail in previous
183 studies (Mozaffar et al., 2020; Zhang et al., 2021b). The decomposition of the PMF
184 mass balance equations is simplified as follows (Norris et al., 2014):

185

186
$$x_{ij} = \sum_{k=1}^{p} g_{ik} \, f_{kj} + e_{ij} \qquad (1)$$

187

188 where x_{ij} is the mass concentration of species j measured in sample i; g_{ik} is the
189 contribution of factor k to the sample i ; f_{kj} represents the content of the jth species in
190 factor k; e_{ij} is the residual of species j in sample i; p represents the number of factors.
191 The fitting objective of the PMF model is to minimize the function Q to obtain the
192 factor contributions and contours. The formula for Q is given in Eq. (2):

193

$$Q = \sum_{i=1}^{n} \sum_{j=1}^{m} \left[\frac{x_{ij} - \sum_{k=1}^{p} g_{ik} f_{kj}}{u_{ij}} \right]^2 \qquad (2)$$

194

195

196 where n and m denote the number of samples and VOC species, respectively.

197   Concentrations and uncertainty data are required for the PMF model. In this study,

198 the median concentration of a given species is used to replace missing values with an

199 uncertainty of four times of the median values; data less than the Method Detection

200 Limit (MDL) were replaced with half the MDL, with an uncertainty of 5/6 of the MDL;

201 and the uncertainty for values greater than the MDL was calculated using Eq. (3). In

202 Eq. (3), EF is error fraction, expressed as the precision of VOCs species, and the setting

203 range can be adjusted from 5 to 20% according to the concentration difference (Buzcu

204 et al., 2006; Song et al., 2007); and c_{ij} is the concentration of species j in sample i:

205
$$U_{ij} = \sqrt{\left(EF \times c_{ij}\right)^2 + (0.5 \times MDL)^2} \qquad (3)$$

206   when the concentration of VOCs in the species is less than the value of the

207 detection limit U_{ij} is calculated using Eq. (4):

208
$$U_{ij} = \left(\frac{5}{6}\right) MDL \qquad (4)$$

209   VOC species and concentration input into PMF were carefully selected to ensure

210 the accuracy of the PMF results. Species were excluded when over 25% of the samples

211 were missing or concentrations values were below the MDL (Gao et al., 2018); VOCs

212 with a short lifetime in the atmosphere were also excluded unless they are source-

213 relative species (Zhang et al., 2014; Shao et al., 2016). After that, retained VOC species

214 were categorized according to the signal-to-noise ratio (S/N) with S/N < 0.2 species

215 categorized as bad, 0.2 < S/N < 2 species categorized as weak; and S/N > 2 species

216 categorized as strong (Shao et al., 2016).

217   We used displacement of factor elements (DISP) to assess PMF modelling

218 uncertainty (for a description, see Paatero et al. (2014)). Q was less than 1% and no

219 swaps occurred for the small est dQ^{max} in DISP. Fpeak values from -2 to 2 were tested

220 to explore the rotational stability of the solutions. Q_{true}/Q_{exp} is lowest when Fpeak = 0,

221 so we chose the PMF results for that case (Fig. S2a). After examining 3-8 factors, 20

222 base runs with 5 factors eventually selected to represent final result. We provide an

223 explanation of factor selection in the supplementary materials. Fig. S2(b) includes

224 Q_{true}/Q_{exp}, Q_{robust}/Q_{exp} for factors 3-8. The slopes of these two ratios in changed at five

225   factors, and we found that five factors were more realistic after repeated comparisons

226   of the results at four, five and six factors.

227 2.3 SOA generation potential

228   The contributions of VOC species to SOAP were calculated based on the toluene

229   weighted mass contributions (TMC) method (Derwent et al., 2010). The methodology

230   for calculating SOAP is as follows:

231

$$232 \quad SOAPF_i = \frac{VOCs\ component\ i\ to\ SOA\ mass\ concentration\ increments}{Toluene\ to\ SOA\ mass\ concentration\ increment} \times 100 \quad (5)$$

233

234        $SOAPF_i$ for each VOC is taken from the literature (Derwent et al., 2010). The

235   SOAP was estimated by multiplying the $SOAPF_i$ value by the concentration of

236   individual VOC species. The SOAP calculations through each VOC are as follows:

237

$$238 \quad SOAP = \sum E_i \times SOAPF_i \quad (6)$$

239   E_i is the concentration of species i.

240

241 3.   Results and discussion

242 3.1 Overview of variation in pollutants and meteorological

243 parameters

244   Figure 1 shows the time series of meteorological parameters, TVOCs, O_3, NO_x,

245   SO_2, CO and $PM_{2.5}$ during the observed periods. Low WS and Temperature were found

246   with an average value of 1.3 ± 0.6 m/s and 5.0 ± 2.5 °C, respectively, during the entire

247   period, comparable with observations at the same site in 2021 (Lai et al., 2024). A total

248   of 62 days of valid data was acquired with the daily average concentration of $PM_{2.5}$

249   ranging from 53 to 239 $\mu g/m^3$, with the average value of 111 ± 45 $\mu g/m^3$. The

250   concentration of TVOCs ranged from 15.6 to 57.1 ppbv with an average of 36.1 ± 21.0

251   ppbv, higher than the same period in last year (27.9 ± 12.7 ppbv, Lai et al., 2024).

252   During the observation period, the average values of T, WS and RH were 5.0 ± 2.5 °C,

253   1.3 ± 0.6 m/s and $38.9 \pm 16.7\%$, respectively.

254   Previous studies have shown that meteorological factors such as low WS, high RH,

and low precipitation are responsible for the increase in $PM_{2.5}$ pollution in Zhengzhou in winter (Duan et al., 2019). Our analysis of the correlation between different pollutants and meteorological conditions during the pollution period showed that $PM_{2.5}$, TVOCs and NO_x were positively correlated with relative humidity (Fig. S3), which is consistent with the results of some previous studies (Wang et al., 2019). Yu et al. (2018) identified RH and WS as the most influential meteorological conditions of $PM_{2.5}$ during winter. Their findings revealed a positive correlation between hourly $PM_{2.5}$ concentrations and RH ($r = 0.84$, $p < 0.01$) and a negative correlation between $PM_{2.5}$ concentrations and WS ($r = -0.62$, $p < 0.01$). In this study, the WS on clean days (1.4 ± 0.8 m/s) was higher than in Case 1 (1.2 ± 0.9 m/s) and Case 2 (0.9 ± 0.7 m/s), while the RH was lower by 26.2% and 12.5% compared to Case 1 and Case 2, respectively. These findings indicate that high RH and low WS significantly influence the occurrence of pollution during the observation period. However, the mean $PM_{2.5}$ concentration during the recovery period was found to be 1.6 times higher than that observed during the infection period. Furthermore, the concentrations of other pollutants (including SO_2, NO_2, CO, and O_3) exhibited analogous trends during the infection and recovery periods. The concentration of TVOCs during the recovery period was 1.2 times higher than that during the infection period, exhibiting a significant upward trend following the resumption of production. It is notable that WS, which is only 0.3 m/s higher in Case 1 than in Case 2, and RH, which is 13% higher in Case 1 than in Case 2, were relatively stable, while the concentration of pollutants is significantly higher in Case 2 than in Case 1. This is presumably attributable to the resumption of production activities in Case 2, which resulted in a notable increase in emissions. Decreased trends of air pollutants were found in other studies before and after the outbreak of the novel coronavirus (COVID-19) in early 2020 (Qi et al., 2021; Wang et al., 2021).
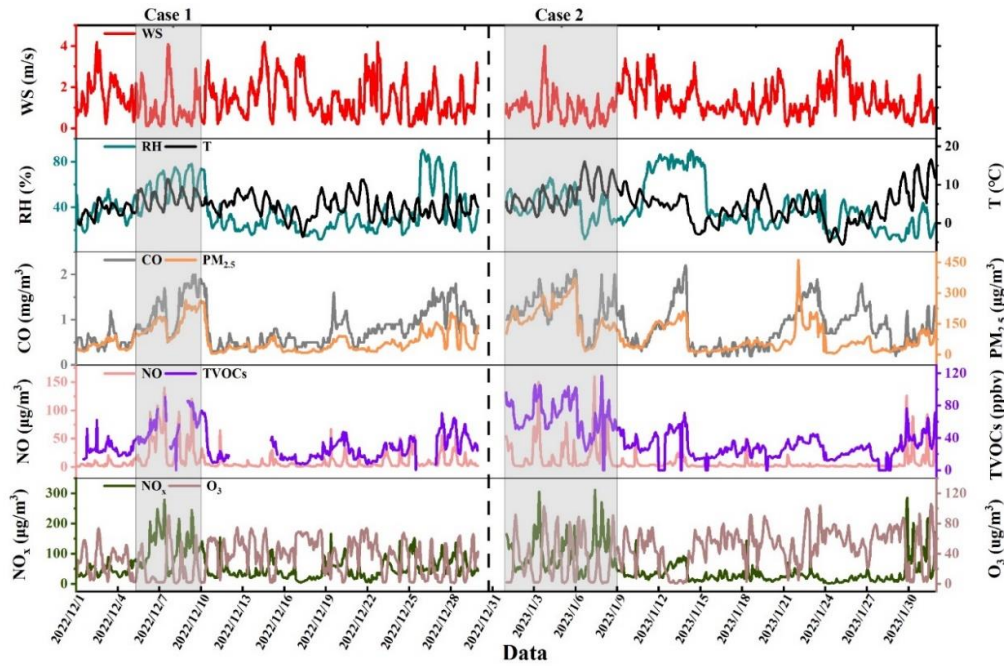
281

282   Fig. 1. Time series of WS, T, RH, CO, PM$_{2.5}$, NO, TVOCs, NO$_x$ and O$_3$ during the observation

283   period.

284   The shadow section in Fig. 1 represents two haze pollution events during the

285   monitoring period. A pollution event is determined when the daily average

286   concentration of PM$_{2.5}$ exceeds 75 μg/m^3 (China's II-level standard) for at least three

287   consecutive days. Case 1 (December 5 to December 10 with daily average PM$_{2.5}$ =

288   142.5 μg/m^3) and Case 2 (January 1 to January 8 with daily average PM$_{2.5}$ = 181.5

289   μg/m^3) were selected as they represent the pollution events in infection and recovery

290   periods, respectively, due to their long duration and high pollution levels. Any day with

291   a PM$_{2.5}$ concentration lower than 35 μg/m^3 (China's I-level standard) is considered as

292   Clean day.
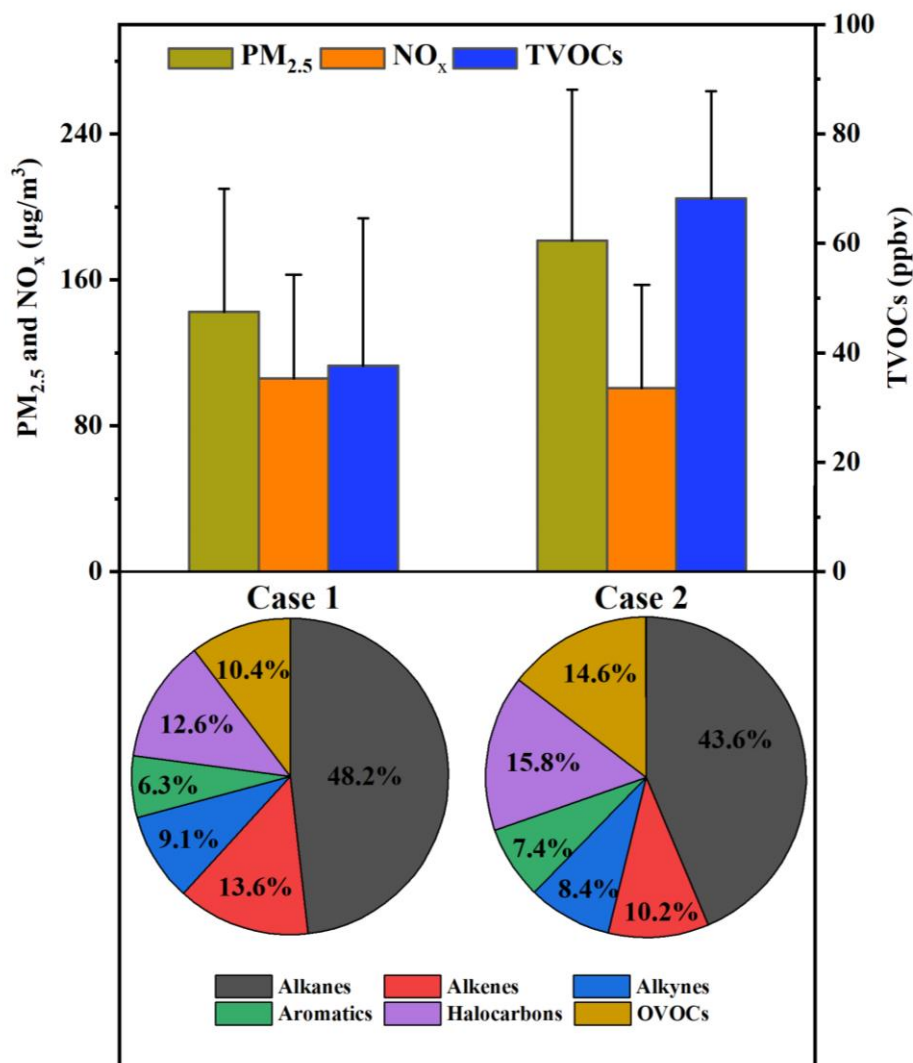
Fig. 2. The concentration of $PM_{2.5}$, NO_x, TVOCs and the composition ratio of VOCs in Case 1 and Case 2.

As for the two representative pollution processes (Case 1 during the infection period and Case 2 during the recovery period), the concentration of TVOCs in Case 1 and Case 2 were 48.4 ± 20.4 and 67.6 ± 19.6 ppbv (Fig. 2), respectively, increased by 63% and 188% compared with values during clean days. The average concentrations of $PM_{2.5}$ and TVOCs during Case 2 were 1.3 and 1.8 times the values in Case 1. The highest volume contributions of alkanes were found both in Case 1 (48%) and Case 2 (44%), consistent with the results in the Yangtze River Delta region (36-43%, Liu et al., 2023). While alkenes exhibited higher volume percentages of 13% in Case 1, followed by halogenated hydrocarbon (12%) and OVOCs (10%). Higher volume percentages of alkanes and alkenes in Case 1 were similar to the results in the gasoline evaporation site in winter (Niu et al., 2022). Equivalent volume contribution of halogenated hydrocarbon and OVOCs (15%) were found in Case 2, followed by alkenes (10%).

308   Although aromatic hydrocarbons have the lowest volumetric contribution (6% in Case

309   1 and 7% in Case 2), they show the largest increase from clean days to pollution.

310   Table 1 The average concentrations of meteorological parameters and pollutants during different

311   processes.

Category	Entire process (2022.12.1-2023.1.31)	Infection period (2022.12.1-2022.12.31)	Recovery period (2023.1.1-2023.1.31)	Case 1 (2022.12.5-2022.12.10)	Case 2 (2023.1.1-2023.1.8)	Clean Days
	N = 62 days	N = 31 days	N = 31 days	N = 6 days	N = 8 days	N = 8 days
WS (m/s)	1.3 ± 0.6	1.4 ± 0.6	1.3 ± 0.6	1.2 ± 0.9	0.9 ± 0.7	1.4 ± 0.8
T (°C)	5.0 ± 2.5	4.7 ± 1.7	5.4 ± 3.1	6.1 ± 2.2	7.4 ± 3.5	4.1 ± 3.0
RH (%)	38.9 ± 16.7	37.6 ± 15.5	40.2 ± 18.2	55.7 ± 14.7	42.0 ± 12.1	29.5 ± 18.1
TVOCs (ppbv)	36.1 ± 21.0	31.9 ± 18.1	39.8 ± 22.4	37.6 ± 27.0	68.2 ± 19.6	22.7 ± 11.1
SO_2 (μg/m^3)	11.4 ± 2.7	10.2 ± 2.8	12.7 ± 2.3	11.0 ± 3.7	16.2 ± 6.1	6.5 ± 2.5
NO_2 (μg/m^3)	47.2 ± 10.0	46.8 ± 8.6	47.8 ± 11.7	62.7 ± 20.5	65.0 ± 21.3	20.8 ± 15.9
CO (mg/m^3)	0.9 ± 0.2	0.8 ± 0.2	1.1 ± 0.2	1.2 ± 0.5	1.3 ± 0.4	0.5 ± 0.2
O_3 (μg/m^3)	34.9 ± 6.0	31.1 ± 4.5	39.0 ± 4.6	21.8 ± 23.7	32.5 ± 29.6	52.6 ± 18.4
$PM_{2.5}$ (μg/m^3)	111.5 ± 45.1	86.6 ± 34.6	138.3 ± 39.6	142.5 ± 67.4	181.5 ± 82.7	23.8 ± 16.8

312   Table 2 Concentration of VOC species during different processes (ppbv).

Category	Entire process	Infection period	Recovery period	Case 1	Case 2	Clean days
TVOCs	36.1 ± 21.0	31.9 ± 18.1	39.8 ± 22.4	48.4 ± 20.4	67.6 ± 19.6	17.5 ± 9.5
alkanes	16.8 ± 9.2	15.0 ± 8.4	18.4 ± 9.5	23.1 ± 10.0	29.5 ± 8.4	9.2 ± 5.6
alkenes	4.1 ± 2.7	3.8 ± 2.6	4.4 ± 2.7	6.5 ± 2.9	7.0 ± 2.6	1.7 ± 1.3
alkynes	3.1 ± 2.0	2.7 ± 1.7	3.4 ± 2.1	4.3 ± 2.0	5.8 ± 1.9	1.3 ± 0.8
aromatics	2.1 ± 2.0	1.8 ± 1.5	2.3 ± 2.2	3.0 ± 1.8	4.9 ± 2.8	0.7 ± 0.5
halogenated hydrocarbon	5.4 ± 3.3	4.4 ± 2.3	6.2 ± 3.8	6.0 ± 1.9	10.7 ± 3.6	2.7 ± 1.4
OVOCs	4.6 ± 3.2	3.5 ± 2.7	5.1 ± 3.5	5.0 ± 2.4	9.7 ± 2.8	1.9 ± 1.1

313   **3.2 Source Analysis of VOCs**

314   Specific VOC ratios can be used for initial source identification of VOCs and

315   determination of photochemical ages of air masses (Monod et al., 2001; An et al., 2014;

316   Li et al., 2019). In this study, the ratios of toluene/benzene (T/B), isopentane/n-pentane,

317   isobutane/n-butane, and m/p-xylene/ethylbenzene (X/E) were selected to initially

318   identify the potential sources of VOCs (Fig. 3). Concentrations of selected pollutants

319   and ratios used are shown in Table S1.

The toluene-to-benzene ratio (T/B ratio) was widely used to assess the relative importance of different sources. Specifically, T/B ratio with a value of 1.3-3.0 was observed in vehicle emissions for vehicles with different fuel types (Schauer et al., 2002; Wang et al., 2015). The reported T/B ratio for combustion processes was between 0.13 and 0.7 (Li et al., 2011; Wang et al., 2014). The mean value of T/B ratio for the entire period was 1.0, with the majority of the data (99%) falling between 0.1 and 3.0 and concentrated within the 0.7-1.3 range (49%). This suggests that both traffic emissions and combustion may be significant sources of VOCs.

The isopentane/n-pentane concentration ratios of 0.6-0.8 represent mainly coal combustion emissions, ratios of 0.8-0.9 represent LPG emissions, 2.2-3.8 represent vehicle exhaust emissions, and 1.8-4.6 represent fuel evaporation (Conner et al., 1995; Liu et al., 2008; Li et al., 2019). The sources of isopentane and n-pentane in this study were intricate and multifaceted. The mean isopentane/n-pentane ratio was 1.4, with the majority of data points (99%) falling within the range of 0.1-4.6, with a notable concentration in the 0.8 to 1.8 interval. This indicates that pentane is susceptible to a combination of LPG emissions and fuel evaporation. It should be noted that this analytical approach is not without limitations. For instance, the proportionality of pentane may be influenced by a combination of LPG emissions and fuel evaporation. Consequently, an in-depth examination of the sources of VOCs was conducted using the PMF model in the next section.

Isobutane/n-butane concentration ratios of 0.2-0.3 represent vehicle emissions, 0.4-0.6 represent LPG usage, and 0.6-1.0 represent natural gas emissions (Russo et al., 2010; Zheng et al., 2018). The mean isobutane/n-butane ratio in this study was 0.5, with the majority of data points (99%) falling within the 0.4-0.6 range, indicating that VOCs at the observation sites were significantly influenced by the use of LPG. (Shao et al., 2016; Zeng et al., 2023).

The ratio of X/E can be used to infer the photochemical age of the air mass. X/E ratios around 2.5-2.9 are typical of urban areas, indicating that VOCs are mainly from the urban area (fresh air mass) (Kumar et al., 2018). When this ratio is significantly lower than 3.0, it indicates that VOCs are mainly transported from distant sources (aging air masses) (Kumar et al., 2018). The average X/E value in this study was 2.0 (Fig. 3(d)), indicating low photochemical activity and aging of the air mass at the observation site. Potential source analyses also indicate that air masses are affected by long-range transport (Fig. S4).

354
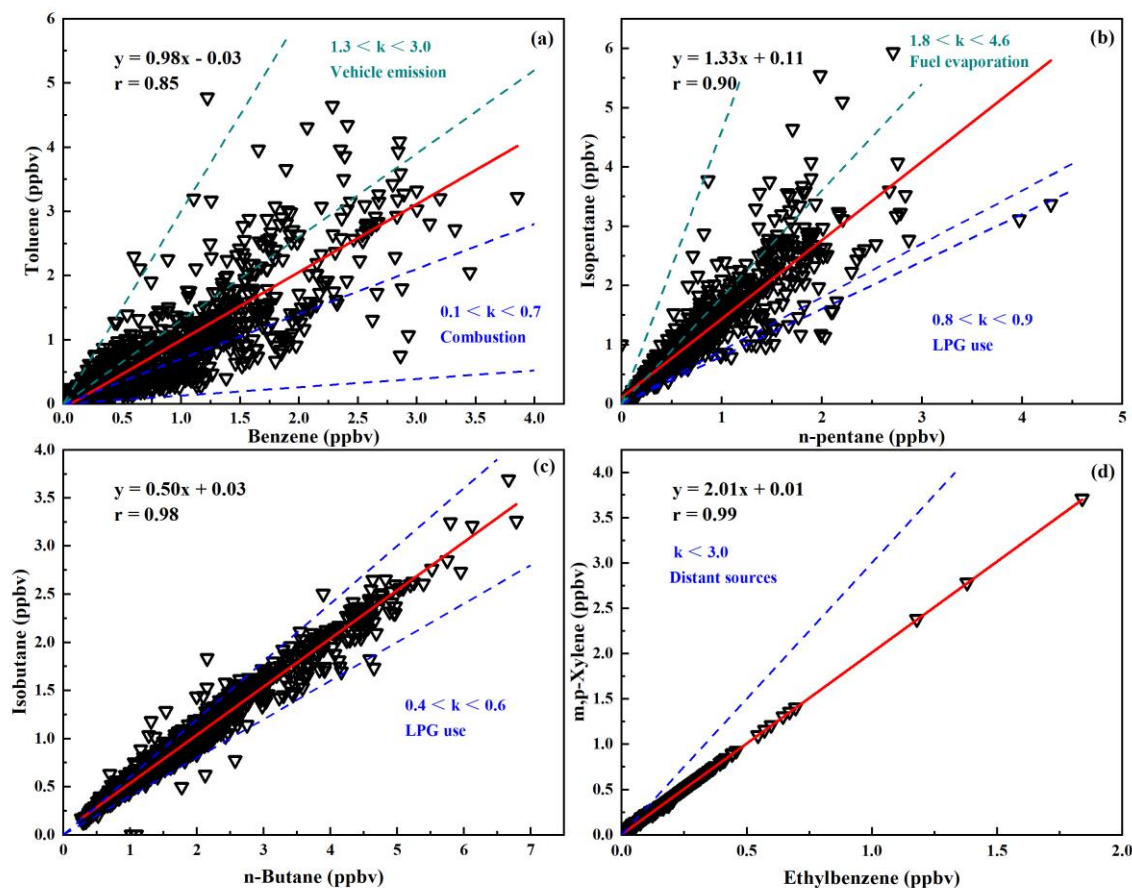
Fig. 3. Correlation analysis between specific VOC species.

Figure 4 shows the chemical profiles of individual VOCs resolved by the PMF model during the entire observation period. These five factors eventually selected as potential sources for the observed VOCs are: (1) Fuel evaporation; (2) Solvent usage; (3) Vehicular emission; (4) Industrial source; and (5) Combustion. These 5 factors have been commonly reported before, e.g., in Shijiazhuang, northern China (Guan et al, 2023) and in Beijing (Cui et al., 2022).

Alkanes of C4-C6 substances were predominant in factor 1, including 2-methylpentane, 3-methylpentane, isobutane, n-butane, isopentane and n-pentane from oil and gas (Xiong et al., 2020). Fig. S5 shows that emissions from this source peak at midday, when fuel volatilization is high, The CPF plot shows that south-east is the dominant direction at wind speeds of less than 2 m/s (Fig. 5a). Therefore, factor 1 was identified as the source of oil and gas volatilization.

The contribution of benzene, toluene, methylene chloride, 1,2-dichloroethane and ethyl acetate was high in factor 2. It has been shown that benzene, toluene, ethylbenzene, and xylene is an important component in the use of solvents (Li et al., 2015); methylene

chloride is often used as a chemical solvent, while esters are mostly used as industrial solvents or adhesives (Li et al., 2015). Factor 2 is determined to be solvent usage source. The CPF plot shows that due east is the main emission direction at wind speeds less than 2 m/s and southeast is the main source at wind speeds greater than 2 m/s (Fig. 5b).

Factor 3 contains predominantly C3-C8 alkanes, olefins and alkynes, and relatively high concentrations of benzene. These substances are usually emitted by industrial processes (Shao et al., 2016), so Factor 4 is defined as an industrial source. The CPF plots indicate that a local source at low wind speeds is the dominant sources (Fig. 5c).

Factor 4 is characterized by relatively high levels of C2-C6 low-carbon alkanes (ethane, propane, isopentane, n-pentane, isobutane and n-butane), olefins (ethylene and propylene), and benzene and toluene, which are important automotive exhaust tracers (Song et al., 2021; Zhang et al., 2021b). Ethylene and propylene are important components derived from vehicle-related activities. Previous studies of VOCs in Zhengzhou have shown a high percentage of VOCs emitted from gasoline vehicles, with the main source of alkanes being on-road mobile sources (Bai et al., 2020). The daily variation of this source in Fig. S5 shows a bimodal trend, with peaks occurring in the morning and evening peaks of traffic, consistent with motor vehicle emissions. Fig. 5d shows that this source is mainly from the west where wind speeds are below 2 m/s, and in this direction, there are a number of urban arterial roads with high traffic volumes. Therefore, factor 4 was defined as vehicular emission source.

The highest contribution to factor 5 is chloromethane (62%). Benzene (46%) and acetylene (41%) also contribute highly to factor 5. Chloromethane is the key tracer for biomass combustion and acetylene is the key tracer for coal combustion (Xiong et al., 2020). Therefore, factor 5 is defined as a combustion source. The CPF plot shows that at wind speeds below 2 m/s, the north-east direction is the dominant source direction (Fig. 5e).

398
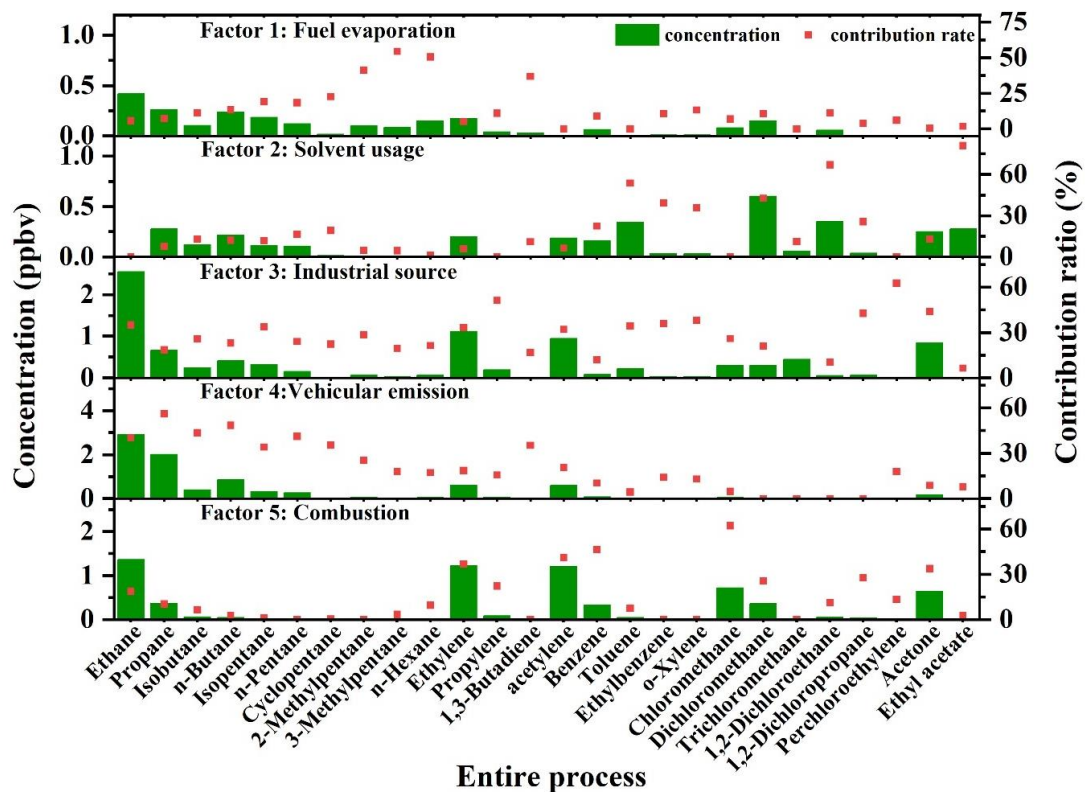
Fig. 4. Concentration of VOC species in each factor and contribution to each source.
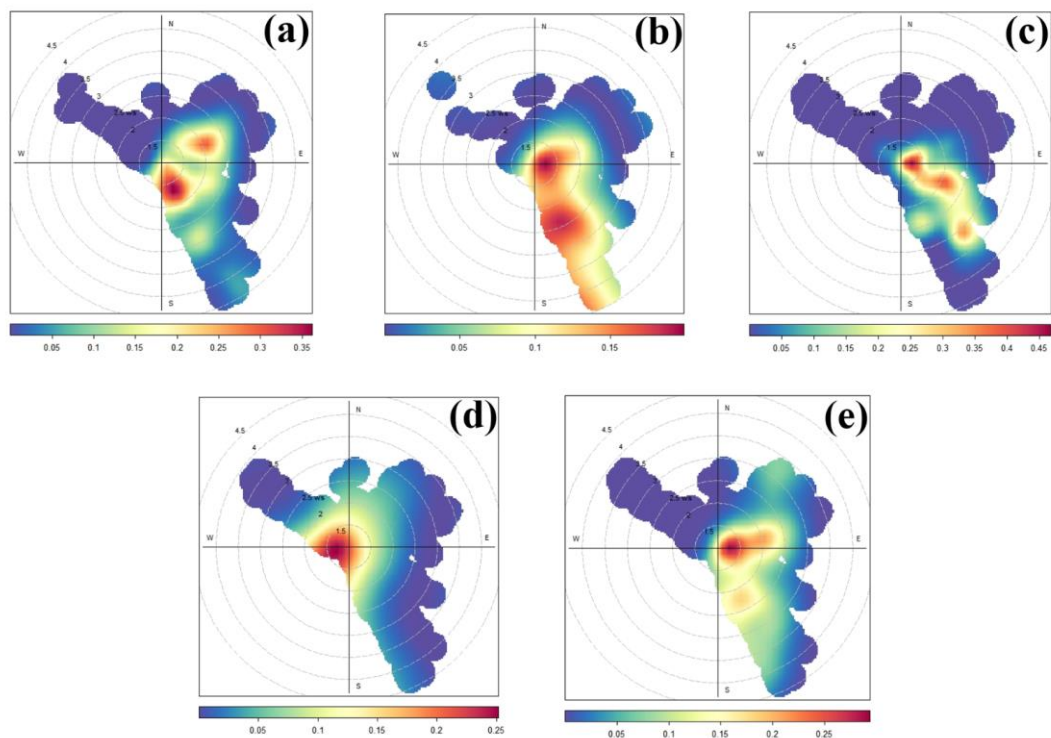
400

401   Fig. 5. CPF plots of five VOCs sources obtained using the PMF model.

Note: a: Fuel evaporation; b: Solvent usage; c: Industrial source; d: Vehicular emission; e: Combustion.

Fig. S6 compares the differences in PMF source profiles between the Omicron infection period and the recovery period, as well as between the pollution day and the clean day. We present the concentrations of the five main VOCs in all five factors in Table S2. Ethane (vehicular emission), 2-methylpentane (fuel evaporation), benzene (industry source), chloromethane (combustion), and ethyl acetate (solvent usage) were selected as tracers for five sources. Ethane concentration in Case 2 (5.9 ppbv) is much higher than in other processes, and ethane concentration during the recovery period (3.4 ppbv) is also higher than during the infection period (2.4 ppbv), which may to some extent reflect increased vehicular emissions during the recovery period.

Concentrations of most species were significantly higher during the recovery period than during the infection period. The representative pollution processes in both periods showed the same results as well, with a 79% higher concentration of TVOCs in Case 2 (65.1 ppbv) compared to Case 1 (36.3 ppbv) (Fig. 6). While in Case 1 industry was the dominant source of VOCs, by Case 2 motorized sources reached a concentration value of 21.2 ppbv, accounting for 33% of the observed VOCs, and became the dominant source of emissions. This is consistent with the fact that people's mobility activities have increased after the epidemic has entered the recovery period. As a group of VOCs species with the highest concentration share, ethane and propane contributed more to the clean days motor vehicle source than other processes, which also resulted in a 34% clean days motor vehicle source share.
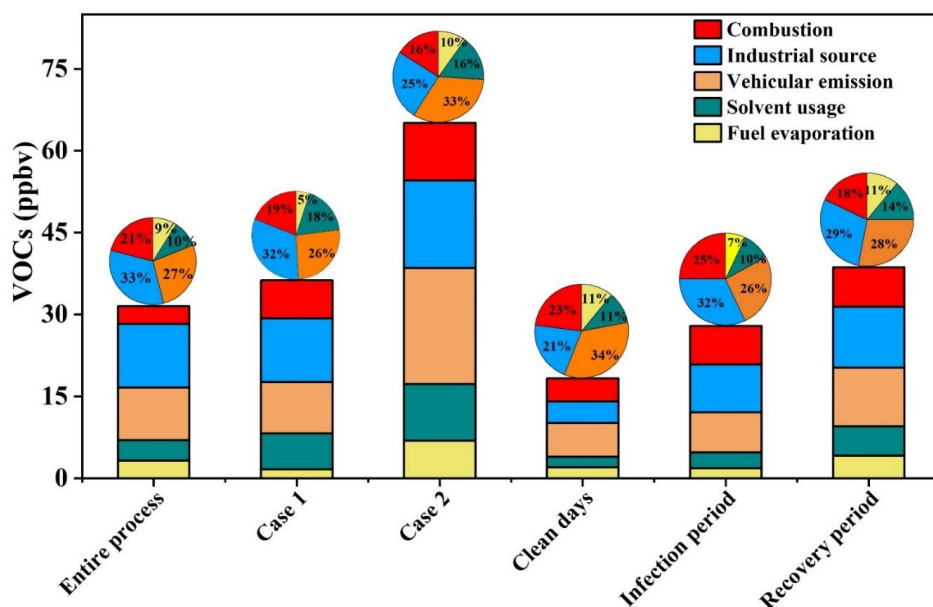
3.3 SOAP

VOCs are estimated to contribute about 16−30% or more of $PM_{2.5}$ by mass through SOA production (Huang et al., 2014). Therefore, by calculating the SOAP value, the influence of different sources on $PM_{2.5}$ production can be reflected to a certain extent.

We have included quantitative analysis for SOAP as well. Fig. 7 shows the SOAP concentrations and contribution rates of the top ten species throughout the entire process, during two pollution processes, and clean days. The top ten species all reached close to 100% of the total SOAP contribution, with Case 1 reaching 98%. In each process, the composition of the top ten substances is essentially the same. Aromatic hydrocarbons contributed the most, with BTEX always occupying the top five positions and toluene the most. The SOAP values of the top ten contributing species for the two polluting processes are shown in Tables S3 and S4. Toluene, the highest contributing species, reached a SOAP value of 49.4 μg/m^3 in the most polluted Case 2, which was 3.2 times higher than the SOAP sum of all species on the clean day (15.5 μg/m^3). The SOAP value for Case 1, which is also a contaminated process, was 67 μg/m^3, and the main species (m/xylene: 9.8 μg/m^3, benzene: 8.5 μg/m^3) including toluene (34.6 μg/m^3) were lower than those for Case 2 (m/xylene: 19.4 μg/m^3, benzene: 13.4 μg/m^3).
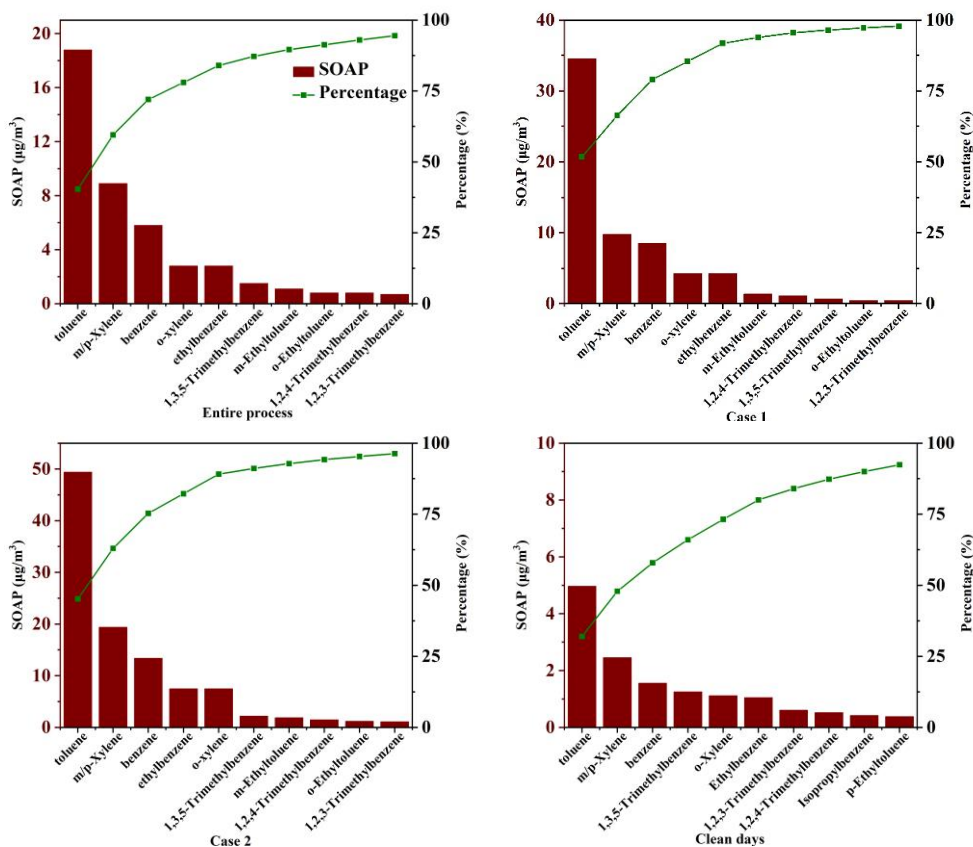
445   Figure 8 shows the SOAP calculated after source resolution of the two pollution

446   processes by PMF for clean days, respectively. In Case 1, industrial source is the

447   dominant source with a contribution ratio of 63%. In Case 2, the pollution sources

448   exhibit a more evenly distributed contribution, where the solvent usage and fuel

449   evaporation sources emerge as the primary contributors to SOAP, with their respective

450   contribution levels rising to 32% and 26%. Case 1 was during the infection period,

451   when social activities had not yet returned to normal. In Case 2, when society had

452   basically returned to normal, the increase in emissions from various sources resulted in

453   a more balanced distribution of SOAP contributions and caused more severe PM$_{2.5}$

454   pollution. In addition, a few days before Case 2, the Zhengzhou Municipal People's

455   Government   initiated   the   Heavy   Pollution   Weather   Level   II   response

456   (https://sthjj.zhengzhou.gov.cn/tzgg/7037130.jhtml) and introduced control measures

457   for emissions from industrial and mobile sources, which resulted in a significant

458   reduction of SOAP levels from industrial and motorized sources in Case 2. The clean

459   day result with a SOAP of 8.8 μg/m^3 also indicates that industrial and solvent usage

460   sources are the most dominant SOAP sources. The primary sources of aromatic

461   compounds, which are the most significant contributors to SOAP, are solvent usage and

462   industrial process emissions. This finding aligns with the results of other studies (Wu

463   et al., 2017). Consequently, it is imperative to implement measures to reduce PM$_{2.5}$

464   pollution by regulating emissions from industrial and solvent usage sources.

465
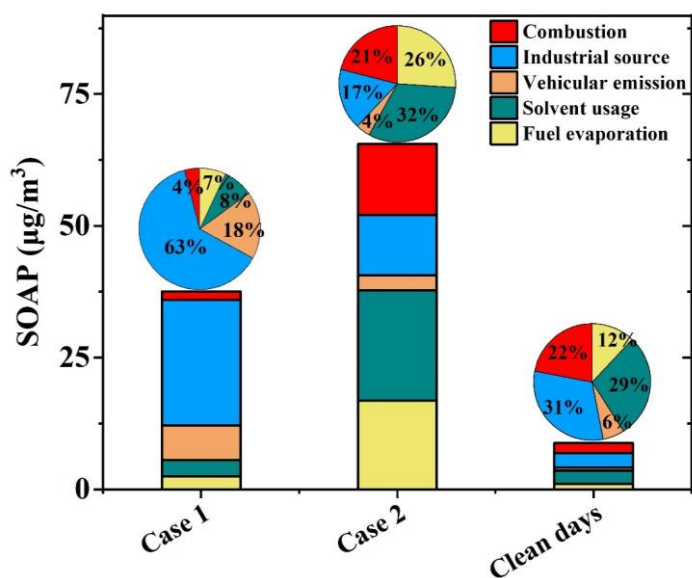
466   Fig. 8. SOAP value and contribution ratio of each process

467

4. Conclusions

Continuous observation of VOCs during the infection of the Omicron epidemic was carried out at an urban site in polluted Zhengzhou from December 1, 2022, to January 31, 2023. The daily average concentration of $PM_{2.5}$ ranged from 53.5 to 239.4 $\mu g/m^3$ with an average value of 111.5 ± 45.1 $\mu g/m^3$ during the whole period. The concentration of TVOCs ranged from 15.6 to 57.1 ppbv with an average of 36.1 ± 21.0 ppbv, higher than the same period in last year (27.9 ± 12.7 ppbv, Lai et al., 2024). Two representative contamination processes were identified (Case 1 during the infection period and Case 2 during the recovery period). The concentration of TVOCs in Case 1 and Case 2 were 48.4 ± 20.4 and 67.6 ± 19.6 ppbv, respectively, increased by 63% and 188% compared with values during clean days. The average concentrations of $PM_{2.5}$ and TVOCs during Case 2 were 1.3 and 1.8 times of the values in Case 1. This is consistent with the observed increase in pollutant emissions following the return to normal social life from the period of Omicron infection. The highest volume contributions of alkanes were found both in Case 1 (48%) and Case 2 (44%). Though the volume contribution of aromatics were the lowest (6% in Case 1 and 7% in Case 2), the highest increase ratio was found from clean days to polluted episodes. Low wind speed and high humidity were the main meteorological reasons for the occurrence of pollution. Analyzing the sources of VOCs revealed that VOCs were found to be affected by a combination of local emissions and regional transport. The primary sources of atmospheric VOCs in Zhengzhou were identified as industrial emissions (32%), vehicle emissions (27%), and combustion (21%). Significant discrepancies were observed in the sources of VOCs between the two pollution processes. In Case 1, industrial emissions constituted the primary source of VOCs, accounting for 32% of the total VOC concentration. In contrast, in Case 2, the proportion of vehicle emissions increased to 33%, representing the primary source of VOCs.

A further analysis of the effect of VOCs on SOA generation reveals that aromatic compounds are the primary contributors to SOAP, with BTEX being the predominant contributor throughout the period. The SOAP values reached 37.6 and 65.6 $\mu g/m^3$ in Case 1 and Case 2, respectively. In Case 1, the greatest contribution to SOAP was made by industrial sources (63%, 23.8 $\mu g/m^3$), while vehicular sources, which constituted the second most important source, accounted for only 18%. In Case 2, the contribution of each VOC source was more evenly distributed, with solvent use sources and fuel

evaporation sources representing the primary contributors to SOAP, accounting for 32% (20.9 μg/m³) and 26% (16.8 μg/m³), respectively. The SOAP result for the clean day was 8.8 μg/m³, with industrial sources and solvent use still being the primary contributors. Therefore, the industrial and solvent use sectors are the predominant sources of pollutants during this observation. The aforementioned results substantiate the considerable impact of elevated emissions from all sources on the exacerbation of pollution following the conclusion of the Omicron infection.

Author contribution:

Bowen Zhang: Data curation, Methodology, Formal analysis, Writing Original Draft.

Dong Zhang: Data curation, Formal analysis, Review & Editing.

Zhe Dong: Data curation, Formal analysis, Review & Editing.

Xinshuai Song: Data curation, Formal analysis.

Ruiqin Zhang: Supervision, Writing-Review & Editing, Funding acquisition.

Xiao Li: Formal analysis, Investigation, Supervision, Writing-Review & Editing.

Competing interests:

The contact author has declared that none of the authors has any competing interests.

Acknowledgments:

This research was supported by the Natural Science Foundation of Henan Province (232300421395) and the National Key Research and Development Program of China (2017YFC0212400).

References

An, J., Zhu, B., Wang, H., Li, Y., Lin, X., and Yang, H.: Characteristics and source apportionment of VOCs measured in an industrial area of Nanjing, Yangtze River Delta, China, Atmospheric Environment, 97, 206-214, https://doi.org/10.1016/j.atmosenv.2014.08.021, 2014.

Bai, L., Lu, X., Yin, S., Zhang, H., Ma, S., Wang, C., Li, Y., and Zhang, R.: A recent emission inventory of multiple air pollutant, $PM_{2.5}$ chemical species and its spatial-temporal characteristics in central China, Journal of Cleaner Production, 269, 122114, https://doi.org/10.1016/j.jclepro.2020.122114, 2020.

Buzcu, B. and Fraser, M. P.: Source identification and apportionment of volatile

organic compounds in Houston, TX, Atmospheric Environment, 40, 2385-2400, https://doi.org/10.1016/j.atmosenv.2005.12.020, 2006.

Conner, T. L., Lonneman, W. A., Seila, R.L.: Transportation-related volatile hydrocarbon source profiles measured in atlanta, Journal of the Air & Waste Management Association, 45 (5), 383-394, https://doi.org/10.1080/10473289.1995.10467370, 1995.

Cui, L., Wu, D., Wang, S., Xu, Q., Hu, R., and Hao, J.: Measurement report: Ambient volatile organic compound (VOC) pollution in urban Beijing: characteristics, sources, and implications for pollution control, Atmospheric Chemistry and Physics, 22, 11931-11944, https://doi.org/10.5194/acp-22-11931-2022, 2022.

Derwent, R. G., Jenkin, M. E., Utembe, S. R., Shallcross, D. E., Murrells, T. P., and Passant, N. R.: Secondary organic aerosol formation from a large number of reactive man-made organic compounds, Science of the Total Environment, 408, 3374-3381, https://doi.org/10.1016/j.scitotenv.2010.04.013, 2010.

Duan, S., Jiang, N., Yang, L., Zhang, R.: Transport Pathways and Potential Sources of $PM_{2.5}$ During the Winter in Zhengzhou, Environmental Science, Jan 8;40(1):86-93, https://doi.org/10.13227/j.hjkx.201805187, 2019.

Gao, J., Zhang, J., Li, H., Li, L., Xu, L., Zhang, Y., Wang, Z., Wang, X., Zhang, W., Chen, Y., Cheng, X., Zhang, H., Peng, L., Chai, F., and Wei, Y.: Comparative study of volatile organic compounds in ambient air using observed mixing ratios and initial mixing ratios taking chemical loss into account – A case study in a typical urban area in Beijing, Science of the Total Environment, 628-629, 791-804, https://doi.org/10.1016/j.scitotenv.2018.01.175, 2018.

Guan, Y., Liu, X., Zheng, Z., Dai, Y., Du, G., Han, J., Hou, L. a., and Duan, E.: Summer O_3 pollution cycle characteristics and VOCs sources in a central city of Beijing-Tianjin-Hebei area, China, Environmental Pollution, 323, 121293, https://doi.org/10.1016/j.envpol.2023.121293, 2023.

Huang, R., Zhang, Y., Bozzetti, C. et al.: High secondary aerosol contribution to p articulate pollution during haze events in China, Nature, 514 (7521), 218−22, https://d oi.org/10.1038/nature13774, 2014.

Hui, L., Liu, X., Tan, Q., Feng, M., An, J., Qu, Y., Zhang, Y., Deng, Y., Zhai, R., a nd Wang, Z.: VOC characteristics, chemical reactivity and sources in urban Wuhan, ce ntral China, Atmospheric Environment, 224, 117340, https://doi.org/10.1016/j.atmose nv.2020.117340, 2020.

565   Jensen, A., Liu, Z., Tan, W., Dix, B., Chen, T., Koss, A., Zhu, L., Li, L., de Gouw,

566   J.: Measurements of volatile organic compounds during the COVID-19 lockdown in

567   Changzhou, China, Geophysical research letters, 48(20), https://doi.org/10.1029/2021

568   GL095560, 2021.

569   Jiang, N., Hao, X., Hao, Q., Wei, Y., Zhang, Y., Lyu, Z., Zhang, R.: Changes in se

570   condary inorganic ions in $PM_{2.5}$ at different pollution stages before and after COVID-1

571   9 control, Environmental Science, 44(5), 2430-2440, https://doi.org/10.13227/j.hjkx.2

572   02206170, 2023.

573   Kumar, A., Singh, D., Kumar, K., Singh, B. B., and Jain, V. K.: Distribution of

574   VOCs in urban and rural atmospheres of subtropical India: Temporal variation, source

575   attribution, ratios, OFP and risk assessment, Science of the Total Environment, 613-614,

576   492-501, https://doi.org/10.1016/j.scitotenv.2017.09.096, 2018.

577   Lai, M., Zhang, D., Yin, S., Song, X., and Zhang, R.: Pollution characteristics,

578   source apportionment and activity analysis of atmospheric VOCs during winter and

579   summer pollution in Zhengzhou City, Environmental Science, 4108, 3500-3510,

580   https://doi.org/10.13227/j.hjkx.202001133, 2024.

581   Li, B., Ho, S. S. H., Gong, S., Ni, J., Li, H., Han, L., Yang, Y., Qi, Y., and Zhao,

582   D.: Characterization of VOCs and their related atmospheric processes in a central

583   Chinese city during severe ozone pollution periods, Atmospheric Chemistry and

584   Physics, 19, 617-638, https://doi.org/10.5194/acp-19-617-2019, 2019.

585   Li, J., Deng, S., Tohti, A., Li, G., Yi, X., Lu, Z., Liu, J., and Zhang, S.: Spatial

586   characteristics of VOCs and their ozone and secondary organic aerosol formation

587   potentials in autumn and winter in the Guanzhong Plain, China, Environmental

588   Research, 211, 113036, https://doi.org/10.1016/j.envres.2022.113036, 2022.

589   Li, J., Xie, S. D., Zeng, L. M., Li, L. Y., Li, Y. Q., and Wu, R. R.: Characterization

590   of ambient volatile organic compounds and their sources in Beijing, before, during, and

591   after Asia-Pacific Economic Cooperation China 2014, Atmospheric Chemistry and

592   Physics, 15, 7945-7959, https://doi.org/10.5194/acp-15-7945-2015, 2015.

593   Li, J., Lu, K., Lv, W., Li, J., Zhong, L., Ou, Y., Chen, D., Huang, X., and Zhang,

594   Y.: Fast increasing of surface ozone concentrations in Pearl River Delta characterized

595   by a regional air quality monitoring network during 2006–2011, Journal of

596   Environmental Sciences, 26, 23-36, https://doi.org/10.1016/S1001-0742(13)60377-0,

597   2014.

598   Liu, Y., Li, X., Tang, G., Wang, L., Lv, B., Guo, X., and Wang, Y.: Secondary

organic aerosols in Jinan, an urban site in North China: Significant anthropogenic contributions to heavy pollution, Journal of Environmental Sciences, 80, 107-115, https://doi.org/10.1016/j.jes.2018.11.009, 2019.

Liu, Y., Shao, M., Fu, L., Lu, S., Zeng, L., and Tang, D.: Source profiles of volatile organic compounds (VOCs) measured in China: Part I, Atmospheric Environment, 42, 6247-6260, https://doi.org/10.1016/j.atmosenv.2008.01.070, 2008.

Liu, Y., Song, M., Liu, X., Zhang, Y., Hui, L., Kong, L., Zhang, Y., Zhang, C., Qu, Y., An, J., Ma, D., Tan, Q., and Feng, M.: Characterization and sources of volatile organic compounds (VOCs) and their related changes during ozone pollution days in 2016 in Beijing, China, Environmental Pollution, 257, 113599, https://doi.org/10.1016/j.envpol.2019.113599, 2020.

Liu, Z., Hu, K., Zhang, K., Zhu, S., Wang, M., and Li, L.: VOCs sources and roles in O_3 formation in the central Yangtze River Delta region of China, Atmospheric Environment, 302, https://doi.org/10.1016/j.atmosenv.2023.119755, 2023.

Li, X., Wang, S., Hao, J.: Characteristics of volatile organic compounds (VOCs) emitted from biofuel combustion in China, Environmental Science, 32, 3515-3521, 2011.

Li, Y., Yin, S., Zhang R., Yu, S., Yang, J., and Zhang, D.: Characteristics and source apportionment of atmospheric VOCs at different pollution levels in winter in an urban area in Zhengzhou, Environmental Science, 4108, 3500-3510, https://doi.org/10.13227/j.hjkx.202001133, 2020.

Ma, Q., Wang, W., Wu, Y., Wang, F., Jin, L., Song, Y., Han, Y., Zhang, R., Zhang, D.: Haze caused by NO_x oxidation under restricted residential and industrial activities in a mega city in the south of North China Plain, Chemosphere, Volume 305, 135489, https://doi.org/10.1016/j.chemosphere.2022.135489, 2022.

Merino, M., Marinescu, M., Cascajo, A., Carretero, J., Singh, D.: Evaluating the spread of Omicron COVID-19 variant in Spain, Future Generation Computer Systems, 149, 547-561, https://doi.org/10.1016/j.future.2023.07.025, 2023.

Monod, A., Sive, B. C., Avino, P., Chen, T., Blake, D. R., and Sherwood Rowland, F.: Monoaromatic compounds in ambient air of various cities: a focus on correlations between the xylenes and ethylbenzene, Atmospheric Environment, 35, 135-149, https://doi.org/10.1016/S1352-2310(00)00274-0, 2001.

Mozaffar, A., Zhang, Y.-L., Fan, M., Cao, F., and Lin, Y.-C.: Characteristics of summertime ambient VOCs and their contributions to O_3 and SOA formation in a

633 suburban area of Nanjing, China, Atmospheric Research, 240, 104923,
634 https://doi.org/10.1016/j.atmosres.2020.104923, 2020.

635 Mu, L., Feng, C., Li, Y., Li, X., Liu, T., Jiang, X., Liu, Z., Bai, H., and Liu, X.:
636 Emission factors and source profiles of VOCs emitted from coke production in Shanxi,
637 China, Environmental Pollution, 335, 122373,
638 https://doi.org/10.1016/j.envpol.2023.122373, 2023.

639 Niu, Y., Yan, Y., Chai, J., Zhang, X., Xu, Y., Duan, X., Wu, J., and Peng, L.: Effects
640 of regional transport from different potential pollution areas on volatile organic
641 compounds (VOCs) in Northern Beijing during non-heating and heating periods,
642 Science of the Total Environment, 836, 155465,
643 https://doi.org/10.1016/j.scitotenv.2022.155465, 2022.

644 Norris, G., Duvall, R., Brown, S., Bai. S. EPA Positive Matrix Factorization (PMF)
645 5.0 Fundamentals and User Guide. U.S. Environmental Protection Agency, Washington,
646 DC, EPA/600/R-14/108 (NTIS PB2015-105147), 2014.

647 Paatero, P., Eberly, S., Brown, S. G., Norris, G. A.: Methods for estimating
648 uncertainty in factor analytic solutions, Atmospheric Measurement Techniques, Volume
649 7, 781-797, https://doi.org/10.5194/amt-7-781-2014, 2014.

650 Pei, C., Yang, W., Zhang, Y., Song, W., Xiao, S., Wang, J., Zhang, J., Zhang, T.,
651 Chen, D., Wang, Y., Chen, Y., Wang, X.: Decrease in ambient volatile organic
652 compounds during the COVID-19 lockdown period in the Pearl River Delta region,
653 south China, Science of The Total Environment, 823, 153720,
654 https://doi.org/10.1016/j.scitotenv.2022.153720, 2022.

655 Petersen, M. S., Í Kongsstovu, S., Eliasen, E. H., Larsen, S., Hansen, J. L., Vest,
656 N., Dahl, M. M., Christiansen, D. H., Møller, L. F., & Kristiansen, M. F.: Clinical
657 characteristics of the Omicron variant - results from a Nationwide Symptoms Survey
658 in the Faroe Islands, International Journal of Infectious Diseases, 122, 636–643,
659 https://doi.org/10.1016/j.ijid.2022.07.005, 2022.

660 Qi, J., Mo, Z., Yuan, B., Huang, S., Huangfu, Y., Wang, Z., Li, X., Yang, S., Wang,
661 W., Zhao, Y., Wang, X., Wang, W., Liu, K., and Shao, M.: An observation approach in
662 evaluation of ozone production to precursor changes during the COVID-19 lockdown,
663 Atmospheric Environment, 262, 118618,
664 https://doi.org/10.1016/j.atmosenv.2021.118618, 2021.

665 Russo, R. S., Zhou, Y., White, M. L., Mao, H., Talbot, R., and Sive, B. C.: Multi-
666 year (2004–2008) record of nonmethane hydrocarbons and halocarbons in New

667 England: seasonal variations and regional sources, Atmospheric Chemistry and Physics,

668 10, 4909-4929, https://doi.org/10.5194/acp-10-4909-2010, 2010.

669   Sahu, L. K., Tripathi, N., Gupta, M., Singh, V., Yadav, R., Patel, K.: Impact of

670 COVID-19 Pandemic lockdown in ambient concentrations of aromatic volatile organic

671 compounds in a metropolitan city of western India, Journal of geophysical research,

672 Atmospheres : JGR, 127(6), https://doi.org/10.1029/2022JD036628, 2022.

673   Schauer, J., Kleeman, M., Cass, G., Simoneit, B.: Measurement of emissions from

674 air pollution sources.5. C_1-C_{32} organic compounds from gasoline-powered motor

675 vehicles,   Environmental   Science   &   Technology,   36,   1169-1180,

676 https://doi.org/10.1021/es0108077, 2002.

677   Shao, P., An, J., Xin, J., Wu, F., Wang, J., Ji, D., and Wang, Y.: Source

678 apportionment of VOCs and the contribution to photochemical ozone formation during

679 summer in the typical industrial area in the Yangtze River Delta, China, Atmospheric

680 Research, 176-177, 64-74, https://doi.org/10.1016/j.atmosres.2016.02.015, 2016.

681   Shi, Y., Liu, C., Zhang, B., Simayi, M., Xi, Z., Ren, J., and Xie, S.: Accurate

682 identification of key VOCs sources contributing to O_3 formation along the Liaodong

683 Bay based on emission inventories and ambient observations, Science of the Total

684 Environment, 844, 156998, 10.1016/j.scitotenv.2022.156998, 2022.

685   Singh, B., Sohrab, S., Athar, M., Alandijany, T., Kumari, S., Nair, A., Kumari, S.,

686 Mehra, K., Chowdhary, K., Rahman, S., Azhar, E.: Substantial changes in selected

687 volatile organic compounds (VOCs) and associations with health risk assessments in

688 industrial   areas   during   the   COVID-19   Pandemic,   Toxics,   11,   165,

689 https://doi.org/10.3390/toxics11020165, 2023a.

690   Singh, B., Singh, M., Ulman, Y., Sharma, U., Pradhan, R., Sahoo, J., Padhi, S.,

691 Chandra, P., Koul, M., Tripathi, P., Kumar, D., Masih, J.: Distribution and temporal

692 variation of total volatile organic compounds concentrations associated with health risk

693 in Punjab, India, Case Studies in Chemical and Environmental Engineering, 8, 100417,

694 https://doi.org/10.1016/j.cscee.2023.100417, 2023b.

695   Song, M., Li, X., Yang, S., Yu, X., Zhou, S., Yang, Y., Chen, S., Dong, H., Liao,

696 K., Chen, Q., Lu, K., Zhang, N., Cao, J., Zeng, L., and Zhang, Y.: Spatiotemporal

697 variation, sources, and secondary transformation potential of volatile organic

698 compounds in Xi'an, China, Atmospheric Chemistry and Physics, 21, 4939-4958,

699 https://doi.org/10.5194/acp-21-4939-2021, 2021.

700   Song, X., Zhang, D., Li, X., Lu, X., Wang, M., Zhang, B., Zhang, R.: Simultaneous

observations of peroxyacetyl nitrate and ozone in Central China during static management of COVID-19: Regional transport and thermal decomposition, Atmospheric Research, Volume 294, 106958, https://doi.org/10.1016/j.atmosres.2023.106958, 2023.

Song, Y., Shao, M., Liu, Y., Lu, S., Kuster, W., Goldan, P., and Xie, S.: Source apportionment of ambient volatile organic compounds in Beijing, Environmental Science & Technology, 41, 4348-4353, https://doi.org/10.1021/es0625982, 2007.

Wang, H., Li, J., Peng, Y., Zhang, M., Che, H., Zhang, X.: The impacts of the meteorology features on $PM_{2.5}$ levels during a severe haze episode in central-east China, Atmospheric Environment, Volume 197, Pages 177-189, ISSN 1352-2310, https://doi.org/10.1016/j.atmosenv.2018.10.001, 2019.

Wang, H., Wang, Q., Chen, J. Chen, C., Huang, C., Qiao, L. Lou, S., Lu, J.: Do vehicular emissions dominate the source of C6–C8 aromatics in the megacity Shanghai of eastern China?, Environmental Science, 27, 290-297, https://doi.org/10.1016/j.jes.2014.05.033, 2015.

Wang, M., Lu, S., Shao, M., Zeng, L., Zheng, J., Xie, F., Lin, H., Hu, K., and Lu, X.: Impact of COVID-19 lockdown on ambient levels and sources of volatile organic compounds (VOCs) in Nanjing, China, Science of the Total Environment, 757, 143823, https://doi.org/10.1016/j.scitotenv.2020.143823, 2021.

Wang, M., Zeng, L., Lu, S., Shao, M., Liu, X., Yu, X., Chen, W., Yuan, B., Zhang, Q., Hu, M., & Zhang, Z.: Development and validation of a cryogen-free automatic gas chromatograph system (GC-MS/FID) for online measurements of volatile organic compounds, Analytical Methods, 6, 9424, https://doi.org/10.1039/C4AY01855A, 2014.

Wang, T., Xue, L., Brimblecombe, P., Lam, Y. F., Li, L., and Zhang, L.: Ozone pollution in China: A review of concentrations, meteorological influences, chemical precursors, and effects, Science of the Total Environment, 575, 1582-1596, https://doi.org/10.1016/j.scitotenv.2016.10.081, 2017.

Wu, R., Li, J., Hao, Y., Li, Y., Zeng, L., and Xie, S.: Evolution process and sources of ambient volatile organic compounds during a severe haze event in Beijing, China, Science of the Total Environment, 560-561, 62-72, https://doi.org/10.1016/j.scitotenv.2016.04.030, 2016.

Wu, W., Zhao, B., Wang, S., and Hao, J.: Ozone and secondary organic aerosol formation potential from anthropogenic volatile organic compounds emissions in China, Journal of Environmental Sciences, 53, 224-237,

735 https://doi.org/10.1016/j.jes.2016.03.025, 2017.

736 Xiong, Y., Zhou, J., Xing, Z., and Du, K.: Optimization of a volatile organic
737 compound control strategy in an oil industry center in Canada by evaluating ozone and
738 secondary organic aerosol formation potential, Environmental Research, 191, 110217,
739 https://doi.org/10.1016/j.envres.2020.110217, 2020.

740 Yu, F., Wang, Q., Yan, Q., Jiang, N., Wei, J., Wei, Z., Yin, S.: Particle size
741 distribution, chemical composition and meteorological factor analysis: A case study
742 during wintertime snow cover in Zhengzhou, China, Atmospheric Research, 202, 140-
743 147, 0169-8095, https://doi.org/10.1016/j.atmosres.2017.11.016, 2018.

744 Yun, L., Li, C., Zhang, M., He, L. and Guo, J.: Pollution characteristics and sources
745 of atmospheric VOCs in the coastal background area of the Pearl River Delta,
746 Environmental Science, 4191-4201, https://doi.org/10.13227/j.hjkx.202101155, 2021.

747 Zeng, X., Han, M., Ren, G., Liu, G., Wang, X., Du, K., Zhang, X., and Lin, H.: A
748 comprehensive investigation on source apportionment and multi-directional regional
749 transport of volatile organic compounds and ozone in urban Zhengzhou, Chemosphere,
750 334, 139001, https://doi.org/10.1016/j.chemosphere.2023.139001, 2023.

751 Zhang, C., Liu, X., Zhang, Y., Tan, Q., Feng, M., Qu, Y., An, J., Deng, Y., Zhai, R.,
752 Wang, Z., Cheng, N., and Zha, S.: Characteristics, source apportionment and chemical
753 conversions of VOCs based on a comprehensive summer observation experiment in
754 Beijing, Atmospheric Pollution Research, 12, 230-241,
755 https://doi.org/10.1016/j.apr.2020.12.010, 2021a.

756 Zhang, D., He, B., Yuan, M., Yu, S., Yin, S., and Zhang, R.: Characteristics,
757 sources and health risks assessment of VOCs in Zhengzhou, China during haze
758 pollution season, Journal of Environmental Sciences, 108, 44-57,
759 https://doi.org/10.1016/j.jes.2021.01.035, 2021b.

760 Zhang, D., Li, X., Yuan, M., Xu, Y., Xu, Q., Su, F., Wang, S., Zhang, R.:
761 Characteristics and sources of nonmethane volatile organic compounds (NMVOCs) and
762 O_3–NO_x–NMVOC relationships in Zhengzhou, China, Atmosphere Chemistry and
763 Physics, 24, 8549-8567, https://doi.org/10.5194/acp-24-8549-2024, 2024.

764 Zhang, F., Shang, X., Chen, H., Xie, G., Fu, Y., Wu, D., Sun, W., Liu, P., Zhang,
765 C., Mu, Y., Zeng, L., Wan, M., Wang, Y., Xiao, H., Wang, G., and Chen, J.: Significant
766 impact of coal combustion on VOCs emissions in winter in a North China rural site,
767 Science of the Total Environment, 720, 137617,
768 https://doi.org/10.1016/j.scitotenv.2020.137617, 2020.

769   Zhang, J., Sun, Y., Wu, F., Sun, J., and Wang, Y.: The characteristics, seasonal

770   variation and source apportionment of VOCs at Gongga Mountain, China, Atmospheric

771   Environment, 88, 297-305, https://doi.org/10.1016/j.atmosenv.2013.03.036, 2014.

772   Zhang, Z., Yan, X., Gao, F., Thai, P., Wang, H., Chen, D., Zhou, L., Gong, D., Li,

773   Q., Morawska, L., and Wang, B.: Emission and health risk assessment of volatile

774   organic compounds in various processes of a petroleum refinery in the Pearl River Delta,

775   China,   Environmental   Pollution,   238,   452-461,

776   https://doi.org/10.1016/j.envpol.2018.03.054, 2018.

777   Zheng, H., Kong, S., Xing, X., Mao, Y., Hu, T., Ding, Y., Li, G., Liu, D., Li, S.,

778   and Qi, S.: Monitoring of volatile organic compounds (VOCs) from an oil and gas

779   station in northwest China for 1 year, Atmospheric Chemistry and Physics, 18, 4567-

780   4595, https://doi.org/10.5194/acp-18-4567-2018, 2018.

781   Zheng, J., Zhong, L., Wang, T., Louie, P. K. K., and Li, Z.: Ground-level ozone in

782   the Pearl River Delta region: Analysis of data from a recently established regional air

783   quality   monitoring   network,   Atmospheric   Environment,   44,   814-823,

784   https://doi.org/10.1016/j.atmosenv.2009.11.032, 2010.

785   Zhou, Z., Xiao, L., Fei, L., Yu, W., Lin M., Huang, T., Zhang, Z. and Tao J.:

786   Characteristics and sources of VOCs during ozone pollution and non-pollution periods

787   in summer in Dongguan industrial concentration area, Environmental Science, 4497-

788   4505, https://doi.org/10.13227/j.hjkx.202111285, 2022.

789   Zou, Y., Yan, X. L., Flores, R. M., Zhang, L. Y., Yang, S. P., Fan, L. Y., Deng, T.,

790   Deng, X. J., and Ye, D. Q.: Source apportionment and ozone formation mechanism of

791   VOCs considering photochemical loss in Guangzhou, China, Science of the Total

792   Environment, 903, 166191, https://doi.org/10.1016/j.scitotenv.2023.166191, 2023.

793   Zuo, H., Jiang, Y., Yuan, J., Wang, Z., Zhang, P., Guo, C., Wang, Z., Chen, Y., Wen,

794   Q., Wei, Y., Li, X.: Pollution characteristics and source differences of VOCs before and

795   after COVID-19 in Beijing, Science of The Total Environment, 907, 167694,

796   https://doi.org/10.1016/j.scitotenv.2023.167694, 2024.

797